Ultra-sensitive DNAzyme-based optofluidic biosensor with liquid crystal-Au nanoparticle hybrid amplification for molecular detection

Ziyihui Wang [1,2], *Yize Liu* [1], *Haonan Wang,*[1] *Shuang Wang* [1], *Kun Liu*[1], *Tianhua Xu* [1, 3*], *Junfeng Jiang* [1*], *Yu-Cheng Chen* [2] and *Tiegen Liu* [1]

1. School of Precision Instrument and Opto-Electronics Engineering
Tianjin University
Tianjin, 300072, China
E-mail: jiangjfjxu@tju.edu.cn

2. School of Electrical and Electronics Engineering
Nanyang Technological University
Singapore 639798, Singapore

3. School of Engineering
University of Warwick
Coventry, CV4 7AL, United Kingdom
E-mail: tianhua.xu@ieee.org

Corresponding authors: Tianhua Xu, Junfeng Jiang

Keywords: liquid crystal, DNAzyme, biosensor, whispering-gallery mode, optofluidic, molecular detection

Abstract

Due to the specific cofactor dependence and the potent catalytic capability, DNAzymes have shown great promise in the application of biosensors. However, it poses significant challenges for researchers to enhance the sensitivities of DNAzyme-based biosensing platforms. In this work, an ultra-sensitive, label-free, and quick-responsive DNAzyme biosensor is developed based on whispering gallery mode (WGM) optofluidic resonator with a hybrid amplification from liquid crystals (LCs) and Au nanoparticles (AuNPs). When a DNAzyme is cleaved by biotargets, the event of DNA hybridization is triggered and will result in the orientation transition of LC molecules (in the resonator core). According to the quadruple amplification from the disturbance of AuNPs, the excess polarizability of adhering biomolecules, the orientation variation of LC molecules, and the WGM resonance, the spectral wavelength shift can be employed as the sensing parameter to indicate the information of biotarget. L-histidine molecules are applied as the analyte. An ultra-low detection limit at a sub-femtomole level (~ 5×10^{-16} M) has been achieved using this highly-selective biosensor, which is eight orders of magnitude lower compared to the reported LC-based L-histidine sensor. In addition to L-histidine, this proposed optofluidic scheme with LC-AuNP hybrid amplification can also extend the applicability of DNAzyme-based biosensors for the detection of various molecules.

1. Introduction

As one branch of catalytic nucleic acids, DNAzymes have the capability of accurate specific substrate recognition and efficient sequence-specific cleavage in the presence of cofactors to activate cleavage reactions[1,2]. Furthermore, DNAzymes exhibit the advantages of low cost as well as high flexibility and chemical stability. These make DNAzymes a promising platform for biosensing. Many research works have shown broad applications of DNAzymes in detecting metal ions,[3-6] small biomolecules[7-9], and bacteria[10], accompanied by investigations on a series of detection methods, e.g. fluorescence, colorimetry, surface-enhanced Raman scattering (SERS), electrochemistry etc.[11] However, previous DNAzyme-based sensors were severely constrained with the low limit of detection (LOD) due to the strong background interference. Therefore, in order to enhance the sensitivity of DNAzyme-based biosensors, it is of great importance to develop a reliable, simple, and quick-responsive approach, that can overcome the environmental interference and can further realize the signal amplification.

The whispering-gallery mode (WGM) is a surface mode, which enables interaction with targets near the surface of the optical resonance based on the extension of the evanescent field and the total internal reflection at the boundary. Taking the merit of high quality factor (Q factor, the ability to store energy), strong evanescent field, and small mode volume,[12] WGM resonators exhibit an outstanding background rejection capability and a high sensitivity. Based on these remarkable advantages, in recent years, WGM resonators have attracted much research attention and have been extensively investigated in the sensing field.[13-15] Such WGM cavities, which can provide strong optical feedback, are held or surrounded by bio-analytes/materials.[16] In addition, as an emerging branch of quickly-responsive, highly-sensitive, and low-cost materials, liquid crystals (LCs) have also been developed to form WGM micro-resonators for the biosensing detection.[17] The subtle molecular events and external stimuli at interfaces are able to trigger the orientation transitions of LC molecules. LC molecules at the

interface can communicate their orientations (within 100 μm[18]) to further enhance the spectral signal responses from WGM sensors. Consequently, LC-amplified WGM biosensors are considered as potential candidates for implementing ultra-sensitive and portable platforms. So far, LC WGM resonators presented in previous studies are mainly formed by LC droplets and LC coated micro-fibers. [13, 15, 19-21] However, with the aspect of LC structures, they are easily affected by (when they are exposed to) the environment (for example, liquid medium evaporation). This prevents applications of LCs in long-term or multiple measurements. Prosperously, LC-filled optofluidic WGM micro-resonator can provide an efficient, stable, and label-free transduction solution with an ultra-high sensitivity for challenging DNAzyme-based biosensors.

In this paper, we developed a DNAzyme-based biosensor employing an LC-AuNP hybrid-amplified optofluidic ring resonator for the biological detection. The microcavity with a sufficiently thin (~ 4 μm) capillary wall can well allow the entry of the WGM to the core, and this can strengthen light-matter interactions. Since DNAzyme is extensively used in biosensing applications, L-histidine molecules, which can specifically cleave the designed DNAzyme, have been employed as an example biotarget to present and characterize the performance of this platform. The capture probe (ssDNA) decorated internal surface of the microcavity can promote a homeotropic orientation of LC molecules (filled in the capillary). With the release of the partial substrate (a fragment of DNAzyme after cleaved by L-histidine), the DNA hybridization is realized and it changes the surface topology. This can trigger the orientation transition of LC molecules. According to the impact of the excess polarizability of biomolecules on the surface and the orientation transition of LC molecules, small variations in L-histidine molecules can be amplified and monitored via the ultra-sensitive wavelength shift of the WGM spectrum. In addition, it has also been demonstrated that AuNPs linked with the partial substrate can further amplify the alignment transition of LCs and the change of the signal in the WGM spectrum. Our results show that the spectral shift scales with the increment of the concentration of biotargets, and L-histidine molecules at a sub-femtomole level (approximately 5×10^{-16}

M) can be detected, which is eight orders of magnitude better compared to the reported record from LC-based L-histidine sensor[22]. This sensing platform, with an ultra-low sensitivity, not only exhibits an excellent selectivity but also provides more parameter adjustment approaches in the application of optical biosensing. Moreover, our biosensor can act as a multi-functional platform and can be extended to detect other molecules (specific to DNAzyme), by simply changing the sequence of DNAzyme. This platform thus offers a promising solution for the label-free molecular detection.

2. Materials and Methods

2.1 Chemicals and materials

In the fabrication of the microfluidic device, the silica capillary was purchased from Polymicro Inc. (#TSP250350). The nematic LCs, 4′-Pentyl-4-biphenylcarbonitrile (5CB, #P11553) and Sodium cyanoborohydride ($NaBH_3CN$, #S105661), used in the experiment, were purchased from Aladdin Co., Ltd. L-histidine(#H0020). L-phenylalanine (#P0010), L-lysine (#L0010), Glycine (#G8200), Sodium chloride (NaCl, #S8210), Tris-HCl buffer (pH=7.4, #T1090), and Sodium dodecylsulfate (SDS, #S8010) were provided by Solarbio Science & Technology, Co., Ltd. L-tryptophan (#L818799), D-histidine (#D810956), 2X Saline Sodium Citrate Buffer (2 × SSC, #X861541), Magnesium chloride ($MgCl_2$, #M813763), and AuNPs (particle diameter: 10 nm, #G820969) were purchased from Macklin Biochemical Co., Ltd. Both Tris(2-chloroethyl) Phosphate (TCEP, #T065A) and Dimethyloctadecyl[3-(trimethoxysilyl)propyl]ammoniumchloride (DMOAP, #A-FF032) came from Xianding Biotechnology Co., Ltd. Triethoxysilybutyraldehyde (TEA, #SIT8185.3) was purchased from Gelest, Inc. The designed oligonucleotides (including DNAzyme and the capture probe)[22] were synthesized by Sangon Biotech Co., Ltd. The sequences of oligonucleotides are listed in **Table S1**. The DNAzyme consists of a substrate strand, a polyT sequence and an enzyme sequence, and the rA (a sessile riboadenine, marked in

red) in the DNAzyme denotes the cleavage site. In addition, sections marked in blue in two probes are complementary. A syringe pump (#SPLab01) from Shenchen Precision Pump Co., Ltd. was employed for the liquid injection.

2.2 Preparation of microcavity and fiber taper

According to our previous work,[23] the fabrication of the microcavity (with a shape of the microbubble) can be divided into two steps: (1) Capillary stretching. With the assistance of the oxyhydrogen flame (with a diameter at the centimeter level), the silica capillary was heated and could be further stretched. (2) Capillary expanding. Under the real-time monitoring, the capillary was expanded to a microbubble shape using a smaller hydrogen oxide flame with a diameter of the millimeter-scale and a pressure control device. In addition, the wall thickness of the capillary plays an important role in the signal enhancement, which can be controlled by the capillary stretching length, the pressure in the capillary, the outer diameter of the microcavity, and the size of the flame. Herein, the microcavity resonator with an outer diameter of 190 μm and a wall thickness of 4 μm was obtained (**Figure S1(a)**). To realize the evanescent field coupling, the fiber taper with a waist diameter of 1~2 μm was produced employing the flame heating-stretching technique.

2.3 Internal surface of the microcavity treatment and functionalization

To produce the original homeotropic alignment of LC molecules, the microcavity was treated by 0.5% (v/v) DMOAP solution at RT for 10 mins, and was cleaned with the deionized water for 1 min. Then, an aqueous solution containing 1% (v/v) TEA and 0.5% (v/v) DMOAP at 55 °C was used to decorate the internal surface (to help immobilize capture probes) for 1 h, and the microcavity was rinsed with the deionized water again. For the immobilization on the surface, capture probes were dissolved in a 20 mM Tris–HCl buffer solution (pH= 7.4), which contains 100 mM $MgCl_2$ and 10 mM $NaBH_3CN$. After the incubation at 37 °C for 2 h, the buffer solution (2 × SSC) including 0.1% (v/v)

SDS was used to eliminate non-bonded capture probes. 100 mM glycine was injected into the microcavity to block the excess aldehyde group sites subsequently.

2.4 Hybridization between capture probe and AuNPs-modified DNAzyme

At first, through a typical salt-aging protocol,[24, 25] thiolated DNAzymes attached with AuNPs were synthesized by derivatizing an AuNPs solution with DNAzymes (including 5 μM TCEP). After standing for 24 h, 100 mM NaCl was stepwise added to the DNAzyme-AuNP conjugates for another 40 h. Excess reagents were removed via a centrifuging operation at 8000 rpm for 20 mins, and then the DNAzyme/AuNP mixture was dispersed in 10 mM Tris-HCl buffer (pH=7.4, containing 50 mM NaCl and 5 mM $MgCl_2$). Next, various concentrations of L-histidine were added into the above DNAzyme-AuNP conjugates (100 nM), and they were employed to functionalize the microcavity surface immobilized with the capture probe at RT for 1 h. Finally, the unbonded probes were washed by the buffer solution (2 × SSC) including 0.1% (v/v) SDS.

2.5 LC optofluidic biosensor for L-histidine detection

A lower flow rate of LCs can help enhance signals from the variation of LCs in the biomolecular detection. [26] In this study, LCs were injected into the DNAzyme-modified microcavity with a speed of 0.7 μL/min to ensure an efficient molecular interaction. After the arrival of LCs, UV glue was used to seal both ends of the capillary to keep the balance of the air pressure and to mitigate the impact of LC flow on the spectrum. Then the recording of the WGM spectrum was started 10 s later.

2.6 Optical setup

To capture polarized images, the microcavity was sandwiched by two cross polarizers, and a microscope (Coic DSZ2000X) with a charge-coupled device camera (Obvious U3CCD) was used. For the optofluidic biosensing platform, the input laser beam, ranging from 1565 nm to 1580 nm, generated by a tunable laser (Keysight 81607A),

was coupled into the optofluidic resonator. The output spectral signal was received by a powermeter (Keysight 81636B).

3. Results and Discussions

3.1 Principle and Design of the DNAzyme-based Sensor with LC-AuNP Hybrid Amplification

In our work, a simple and specific DNAzyme-based sensor for the L-histidine detection (as a proof-of-concept) is developed, based on the DNA hybridization, the reorientation of LC molecules and the AuNP amplification. (1) DNA hybridization. A substrate strand (from the DNAzyme) containing a ribo-adenine (rA, the recognition site) can be cleaved by L-histidine and was broken into two sections, as seen in **Figure 1(a)**. Then, the fragment, called partial substrate and linked with AuNPs, can dissociate from the DNAzyme and hybridize with the capture probe (ssDNA, a complementary strand decorated on the internal surface of the microcavity) to form the dsDNA on the glass surface. (2) LC sensing. LCs, as a branch of potential materials, are sensitive to the interfacial variation. Reported studies have demonstrated that the surface topology can affect the orientation transition of LC molecules[27]. DMOAP/TEA (with alkanes) decorated on the internal surface of the microcavity can form a self-assembly monolayer (SAM) film and can trigger the homeotropic alignment of LCs. Due to the aldehyde groups of TEA, amine-labeled ssDNA can be immobilized on the glass surface through covalent bonds. With appropriate strand length[28] and surface coverage[29] on the surfaces, ssDNA can also contribute to the homeotropic alignment of LC molecules due to its linear and flexible chain (longer than that of LC molecules). By contrast, dsDNA can trigger the planar orientation of LC molecules. Therefore, when L-histidine molecules enter the microcavity, a homeotropic-to-planar orientation transition of LC molecules will occur due to the DNA hybridization (**Figure 1(b)**). (3) AuNPs amplification. In addition, AuNPs linked with the partial substrate can further

disturb the orientation of LC molecules and amplify the signal. Based on the optical anisotropy of LC molecules, under the POM observation, the polarized image of the LC-AuNP hybrid-amplified microcavity varies accordingly. Polarized images under various concentrations of L-histidine can be found in **Figure S1(b)**. According to the variation in these polarized images observed by the naked eye, the concentration higher than 5×10^{-12} M L-histidine can be distinguished. However, for the concentration (of L-histidine) lower than 5×10^{-12} M, it is very difficult to estimate the small variation in the orientation of LC molecules. Therefore, a more sensitive detection method is essential.

With merits of small mode volume, high Q factor, and strong evanescent field from passive WGM cavities, we have implemented a DNAzyme-based and LC-AuNP-hybrid amplificated WGM sensing system to explore a simple, ultra-sensitive, and real-time detection scheme. In **Figure 1(b)**, the microcavity (with the shape of microbubble) can form a WGM optofluidic resonator with the assistance of the fiber taper. To realize the phase matching and the overlap of evanescent electromagnetic fields, a tunable bracket was employed to adjust the gap between the fiber taper and the micro-resonator. A tunable laser was coupled to the optofluidic resonator via the fiber taper (with an ultra-high coupling efficiency), and then the optical signal was received by the powermeter (**Figure S2**). Compared to the WGM resonator formed by the LC droplet,[17] this LC-based biosensing platform is covered by a silica shell to overcome external disturbances (for example, the evaporation of the aqueous solution) and can provide a stable environment for LCs. This is beneficial to long-term or multiple measurements. To characterize this optofluidic, the free spectral range (FSR), as an important parameter of WGM resonator, is measured to be 2.5 nm (**Figure 2(a)**). As illustrated in **Figure 2(b)**, the electromagnetic profile exhibits the light intensity is mainly focused in the LC region (due to the high refractive index of LC molecules), and first-order and second-order polarization modes are formed. According to theoretical calculations of optical modes,[33, 34] WGMs from the optofluidic resonator are well-fitted with the first-order (mode number from 617 to 622), and the second-order (mode number from 605

to 610) TM polarization modes. Owing to stimuli from biological analytes at the interface, the orientation transition of LC molecules will result in the wavelength shift of the WGM spectrum. After the addition of 5×10^{-7} M L-histidine, in **Figure 2(c)**, the shifting behavior of WGM emissions were monitored for 7 mins. An interesting phenomenon is realized that a redshift can be observed in the first 0.5 mins, then valleys show a blue shift tendency until the spectrum becomes steady (we will discuss it in Section 3.3). Correspondingly, the polarized image of LCs also exhibits an orientation transition from homeotropic to planar. This indicates that the optofluidic spectrum can characterize the biotarget information.

3.2 The effect of AuNPs on WGM spectrum signal enhancement

Due to the good biocompatibility and the interaction with biotargets, nanoparticles are widely used in the labeling of biomolecules and the biosensing field. Previous studies have demonstrated that the orientations of LCs are remarkably sensitive to the variation of the interfacial topography.[27, 30] Compared to volumes of L-histidine and DNA chains, AuNPs exhibit a large size (diameters of ~10 nm) and can significantly change the topology of the surface to facilitate the orientation transition of LC molecules. To explore the effect of AuNPs on the WGM spectrum signal enhancement of LC-based biosensors, AuNPs were linked with DNAzyme to characterize and to amplify the event of DNA hybridization between the partial substrate (as the fragment of DNAzyme) and the capture probe. After cleaved by L-histidine, partial substrates bonded with AuNPs dissociate from the DNAzyme and hybridize with the capture probe to form the dsDNA. At first, we exhibited traces of WGM spectral responses in the LC-based microcavity with/without the assistance of AuNPs at the concentration of 5×10^{-7} M L-histidine, as seen in **Figure 3(a)**. The group with AuNPs enhancement triggers a more significant wavelength shift and needs more time to stabilize the spectrum, because the orientation of LC molecules was further disturbed by AuNPs. As shown in **Figure 3(b)**, the total wavelength shifts of WGM spectra (defined as the absolute value of red shift plus the

absolute value of blue shift, details on the calculation of the total wavelength shift in this study can be found in **Figure S3**) under various concentrations of L-histidine (at 5×10^{-7} M, 5×10^{-12} M, and 5×10^{-15} M) were tested and recorded, respectively. For the group without AuNPs, although various and reliable wavelength shifts can be triggered at the concentrations of 5×10^{-7} M and 5×10^{-12} M (for L-histidine), it is difficult to monitor the spectral responses at the extremely low concentration (e.g. 5×10^{-15} M L-histidine). As a comparison, not only the WGM spectrum from AuNPs-amplified LC sensing platform can respond to 5×10^{-15} M L-histidine (a total wavelength shift of 0.19 nm), the spectral shifts also become more significant than groups without the use of AuNPs enhancement, for the same concentration of L-histidine. By changing the topological structure, AuNPs linked with the partial substrate can greatly promote the orientation transition of LC molecules in the micro-resonator, and can thus enhance the scale of the resonant wavelength. It can be found that AuNPs signal amplification technique improved the sensitivity LC-based sensing platforms significantly.

3.3 DNAzyme-based optofluidic biosensor for L-histidine detection

Based on the previous section, here we have also investigated the applicability of DNAzyme-based LC optofluidic biosensors (including AuNPs amplification) for the molecular detection. **Figure 4(a)** describes the spectral response of the LC microfluidic platform with 5×10^{-9} M L-histidine, where a significant wavelength shift can be observed. As a control experiment, when 0 M L-histidine group was applied (**Figure S4**), there was no significant spectral response observed (< 0.1 nm). This indicates that our platform produces a stable and reliable biosensor.

Then we studied the WGM spectral responses of the DNA zyme-based LC microfluidic under different concentrations of L-histidine. As shown in **Figure 4(b)**, traces of WGM spectral wavelength responses with respect to several representative L-histidine concentrations (5×10^{-7} M, 5×10^{-8} M, 5×10^{-9} M, 5×10^{-11} M, 5×10^{-13} M and 5×10^{-16} M) have been monitored, respectively. According to all collected data, WGM spectra were

found to become steady after 6 mins. Herein, we recorded the wavelength shifts for a time period of over 7 mins, to include the equilibrium of LC microfluidics. The red-shift tendency was recorded as a positive number, and the blue-shift tendency was recorded as a negative number. All these concentrations showed similar tendencies, i.e. the red shift at first, then the blue shift. For the WGM micro-resonator, owing to the disturbed effective refractive index, the resonant wavelength can change accordingly, which can be described by the following equation:

$$\Delta\lambda = \frac{\lambda_{res}}{n_{eff}}\Delta n_{eff}$$

On one hand, the resonant wavelength of WGMs is extremely sensitive to the surface dielectric material. For the biomolecular random absorption, the wavelength shift scales proportionally with the biomolecular surface density and the excess polarizability, due to the light-matter interaction. Therefore, with the appearance of L-histidine and DNA hybridization on the surface, the increasing surface atomic thickness and the interaction between the evanescent field of the WGM and biomolecules contribute to the perturbation in the energy of a single-photon resonant state and the initial red shift tendency of spectral responses. On the other hand, it has been demonstrated that the WGM is a transverse magnetic (TM) mode, which is in agreement with the structure of LCs inside the micro-resonator.[31, 32] With the addition of LCs, the DNA hybridization will result in the orientation transition of LC molecules, from homeotropic to planar. It is known that the optical anisotropy leads to two different refractive indices (i.e., the ordinary, n_o, and the extraordinary, n_e). Without L-histidine, the TM mode along the long axis of LC molecules (with the homeotropic alignment, also called the radial alignment) experiences the extraordinary refractive index (for 5CB, n_e= 1.67). In contrast, the DNA hybridization can promote the planar orientation of LC molecules, and the TM mode responds to the ordinary refractive index (for 5CB, n_o= 1.51) during its circulation. According to the orientation transition of LC molecules, the WGM spectral responses follow the variation of the refractive index of LCs, from n_e to n_o, and exhibit a blue shift tendency in the subsequent measurement period. Therefore, these two factors (biomolecular absorption and orientation transition of LC molecules) have

triggered the WGM spectral shift and amplified the event of the appearance of L-histidine. Moreover, according to **Figure 4(b)**, we further find that both the red shift and the blue shift tendencies increase with the concentrations of L-histidine.

Since the red shift and the blue shift occur together in most cases, to monitor the WGM spectral responses derived from various concentrations of L-histidine, it is reasonable to calculate the total wavelength shift. Accordingly, we have recorded total wavelength shifts of WGM spectra with respect to different concentrations of L-histidine, as plotted in **Figure 4(c)**, where X-axis represented the concentration of L-histidine in a logarithmic scale and Y-axis employed a linear scale. It can be found that the total spectral response increased monotonically with the increment of the L-histidine concentration. We also fitted and calculated the calibration curve, which can be used as a calibration reference in the future for L-histidine sensing and quantification (the blue curve in **Figure 4(c)**). The detected maximum wavelength shift is approximately 3.43 nm under 5×10^{-7} M L-histidine. Eventually, the minimum concentration to obtain the observable spectral shift is approximately 0.5 fM (5×10^{-16} M). Compared to conventional POM approaches (with AuNPs amplification), where only 5×10^{-12} M and above can be detected, the limit of detection of our LC based WGM microfluidic system can achieve a sub-femtomole level (per liter) for the detection of L-histidine. This offers an improvement in the detection sensitivity by four orders of magnitude. The difficulty in distinguishing the orientation transition of LC molecules by the naked eye can now be easily overcome by the use of the WGM spectrum. Furthermore, the repeatability and reproducibility characteristics endowed the sensor with the capability of long-term detection of subtle biological signals. As seen in **Figure S5**, different concentrations of L-histidine (5×10^{-7}, 5×10^{-12} and 5×10^{-16} M) were continuously and cyclically monitored via the micro-resonator. Highly repeatable and stable spectral signal responses demonstrated the excellent performance of this sensing platform. Our results have demonstrated that, based on the transduction method of the WGM spectrum, the DNAzyme-based LC optofluidic scheme provides an ultra-sensitive sensing platform for the L-histidine detection. Due to wide applications of DNAzymes, we can envisage

that this sensing approach has great potential in detecting a series of metal ions and neutral molecules.

3.4 Specific detection capability of DNAzyme-based LC optofluidic biosensor

In addition to its extremely high sensitivity, this DNAzyme-based LC sensor also exhibits high selectivity. To demonstrate the anti-interference capability against other biotargets with structures similar to the L-histidine molecule, as displayed in **Figure 5**, we have also investigated the WGM spectral responses of the LC sensor after the addition of D-histidine, L-phenylalanine, L-lysine and L-tryptophan with the same concentration of 5×10^{-7} M (all were diluted from standard samples), respectively. In contrast with 5×10^{-7} M L-histidine, these foreign amino acids cannot lead to a significant wavelength shift, and their effects on the detection of L-histidine are almost negligible.

3.5 Detection of L-histidine in urine samples

To study the practical applicability, diluted urine samples (diluted by 10^5 times) were employed in this developed optofluidic platform, and the concentration of L-histidine under detection can be quantified via the calibration curve shown in **Figure 4(c).** As seen in **Table 1**, L-histidine with a concentration of 672 μM was detected in the original urine sample (i.e., 6.72 nM in the diluted sample), which was consistent with the normal range in the human urine. In addition, L-histidine with concentrations of 1 nM, 5 nM and 50 nM, were added into the diluted urine separately. Recovery rates of 98.7% for 1 nM, 103.2% for 5 nM, and 104.3% for 50 nM have been achieved. These results demonstrated a strong feasibility of this purposed DNAzyme-based biosensor in the detection of real biosamples.

4. Conclusions

In this work, we have developed a DNAzyme-based optofluidic biosensor using LC-AuNP hybrid amplification for detecting biomolecules with ultra-high sensitivity. Along with the DNA hybridization, the orientation transition of LC molecules (from homeotropic to planar) has been investigated. Owing to the dual effect from the excess polarizability of the adhering biomolecules and the orientation variation of LC molecules, the WGM spectral shift will be triggered to amplify and indicate the information of biotargets. The AuNPs linked with DNAzyme can further disturb the alignment of LC molecules, which results in a more significant shift of the spectrum. Herein, L-histidine has been chosen as the biotarget the under test. Results demonstrate that the total wavelength shift shows a sensitive and monotonic performance with the change in the concentration of L-histidine. With a limit of detection of 5×10^{-16} M (L-histidine), this optofluidic biosensing platform can realize the sensitivity at a sub-femtomole level, which means an improvement by four orders of magnitude compared to the sensitivity in the POM method (with AuNPs amplification). It is also verified that this developed biosensor exhibits good selectivity for the L-histidine detection due to the high specificity between the designed DNAzyme and the L-histidine. This sensing platform provides a label-free, quick-response, and highly-sensitive detection solution for analyte analyses. It is expected that the microfluidic sensor with a thinner wall (< 4 μm) could in principle provide even higher sensitivity for the L-histidine detection. To improve the detection efficiency, real-time image processing (e.g. correlation operation) can be employed to replace manual computations and to realize the spectral analyses. In addition, according to wide applications of DNAzyme, this LC-AuNP hybrid-amplified optofluidic transduction platform can also be employed to detect other biomolecules, if they are specific to DNAzyme. We envision that this proposed scheme could provide new solutions in the detection of biomolecules, with a lower limit of detection than that of conventional methods.

Authors' contributions

This paper was mainly written by Z.W., T.X., and J.J. Z.W. and Y.L. developed the testbed. Z.W. and H.W. carried out the optical experiments. S.W., T.X., J.J., and T.L. proposed the research idea and provided useful discussions. K.L., T.X., J.J., Y.C. and T.L. supervised the project and experiments. All authors contributed to the research work and modifications of this manuscript.

Availability of data and materials

Original data are available on request from corresponding authors.

Declarations

There are no competing interests for this paper.

Acknowledgements

The authors would like to thank the support from Nation Science Foundation of China (Grant No. 61735011), China Scholarship Council (Grant No.202006250152) and EU Horizon 2020 Project (Grant No. 101008280).

References

1. Breaker, R. R.; Joyce, G. F., A DNA enzyme that cleaves RNA. *Chemistry & Biology* **1994,** *1* (4), 223-229.
2. Fan, H.; Zhang, X.; Lu, Y., Recent advances in DNAzyme-based gene silencing. *Science China Chemistry* **2017,** *60* (5), 591-601.
3. He, S.; Song, B.; Li, D.; Zhu, C.; Qi, W.; Wen, Y.; Wang, L.; Song, S.; Fang, H.; Fan, C., A Graphene Nanoprobe for Rapid, Sensitive, and Multicolor Fluorescent DNA Analysis. *Advanced Functional Materials* **2010,** *20* (3), 453-459.
4. Tedsana, W.; Tuntulani, T.; Ngeontae, W., A circular dichroism sensor for Ni2+ and Co2+ based on l-cysteine capped cadmium sulfide quantum dots. *Analytica Chimica Acta* **2015,** *867*, 1-8.
5. Ren, W.; Jimmy Huang, P. J.; de Rochambeau, D.; Moon, W. J.; Zhang, J.; Lyu, M.; Wang, S.; Sleiman, H.; Liu, J., Selection of a metal ligand modified DNAzyme for detecting Ni(2). *Biosens Bioelectron* **2020,** *165*, 112285.
6. McGhee, C. E.; Loh, K. Y.; Lu, Y., DNAzyme sensors for detection of metal ions in the environment and imaging them in living cells. *Curr Opin Biotechnol* **2017,** *45*, 191-201.
7. Kong, R. M.; Zhang, X. B.; Chen, Z.; Meng, H. M.; Song, Z. L.; Tan, W.; Shen, G. L.; Yu, R. Q., Unimolecular catalytic DNA biosensor for amplified detection of L-histidine via an enzymatic recycling cleavage strategy. *Anal Chem* **2011,** *83* (20), 7603-7.
8. Liang, J.; Chen, Z.; Guo, L.; Li, L., Electrochemical sensing of L-histidine based on structure-switching DNAzymes and gold nanoparticle-graphene nanosheet composites. *Chem Commun* **2011,** *47* (19), 5476-8.
9. Lu, L.-M.; Zhang, X.-B.; Kong, R.-M.; Yang, B.; Tan, W., A Ligation-Triggered DNAzyme Cascade for Amplified Fluorescence Detection of Biological Small Molecules with Zero-Background Signal. *Journal of the American Chemical Society* **2011,** *133* (30), 11686-11691.
10. Ali, M. M.; Aguirre, S. D.; Lazim, H.; Li, Y., Fluorogenic DNAzyme Probes as Bacterial Indicators. *Angewandte Chemie International Edition* **2011,** *50* (16), 3751-3754.
11. Gong, L.; Zhao, Z.; Lv, Y. F.; Huan, S. Y.; Fu, T.; Zhang, X. B.; Shen, G. L.; Yu, R. Q., DNAzyme-based biosensors and nanodevices. *Chem Commun* **2015,** *51* (6), 979-95.
12. Zheng, Y.; Wu, Z.; Ping Shum, P.; Xu, Z.; Keiser, G.; Humbert, G.; Zhang, H.; Zeng, S.; Quyen Dinh, X., Sensing and lasing applications of whispering gallery mode microresonators. *Opto-Electronic Advances* **2018,** *1* (9), 18001501-18001510.
13. Wang, Z.; Zhang, Y.; Gong, X.; Yuan, Z.; Feng, S.; Xu, T.; Liu, T.; Chen, Y.-C., Bio-electrostatic sensitive droplet lasers for molecular detection. *Nanoscale Advances* **2020,** *2* (7), 2713-2719.
14. Zhu, H.; White, I. M.; Suter, J. D.; Dale, P. S.; Fan, X., Analysis of biomolecule detection with optofluidic ring resonator sensors. *Optics Express* **2007,** *15* (15), 9139-9146.
15. Yuan, Z.; Wang, Z.; Guan, P.; Wu, X.; Chen, Y.-C., Lasing-Encoded Microsensor Driven by Interfacial Cavity Resonance Energy Transfer. *Advanced Optical Materials* **2020,** *8* (7), 1901596.

16. Chen, Y. C.; Fan, X., Biological Lasers for Biomedical Applications. *Advanced Optical Materials* **2019,** *7* (17).
17. Wang, Z.; Xu, T.; Noel, A.; Chen, Y.-C.; Liu, T., Applications of Liquid Crystal in Biosensing. *Soft Matter* **2021**.
18. Xue, C.-Y.; Yang, K.-L., Dark-to-Bright Optical Responses of Liquid Crystals Supported on Solid Surfaces Decorated with Proteins. *Langmuir* **2008,** *24* (2), 563-567.
19. Zhang, Y.; Yuan, Z.; Qiao, Z.; Barshilia, D.; Wang, W.; Chang, G.-E.; Chen, Y.-C., Tunable Microlasers Modulated by Intracavity Spherical Confinement with Chiral Liquid Crystal. *Advanced Optical Materials* **2020**.
20. Duan, R.; Hao, X.; Li, Y.; Li, H., Detection of acetylcholinesterase and its inhibitors by liquid crystal biosensor based on whispering gallery mode. *Sensors and Actuators B: Chemical* **2020,** *308*, 127672.
21. Duan, R.; Li, Y.; He, Y.; Yuan, Y.; Li, H., Quantitative and sensitive detection of lipase using a liquid crystal microfiber biosensor based on the whispering-gallery mode. *Analyst* **2020**.
22. Liao, S.; Ding, H.; Wu, Y.; Wu, Z.; Shen, G.; Yu, R., Label-free liquid crystal biosensor for L-histidine: A DNAzyme-based platform for small molecule assay. *Biosens Bioelectron* **2016,** *79*, 650-5.
23. Jiang, J.; Liu, Y.; Liu, K.; Wang, S.; Ma, Z.; Zhang, Y.; Niu, P.; Shen, L.; Liu, T., Wall-thickness-controlled microbubble fabrication for WGM-based application. *Appl. Opt.* **2020,** *59* (16), 5052-5057.
24. Mirkin, C. A.; Letsinger, R. L.; Mucic, R. C.; Storhoff, J. J., A DNA-based method for rationally assembling nanoparticles into macroscopic materials. *Nature* **1996,** *382* (6592), 607-609.
25. Shen, L.; Chen, Z.; Li, Y.; He, S.; Xie, S.; Xu, X.; Liang, Z.; Meng, X.; Li, Q.; Zhu, Z.; Li, M.; Le, X. C.; Shao, Y., Electrochemical DNAzyme Sensor for Lead Based on Amplification of DNA−Au Bio-Bar Codes. *Analytical Chemistry* **2008,** *80* (16), 6323-6328.
26. Fan, Y. J.; Chen, F. L.; Liou, J. C.; Huang, Y. W.; Chen, C. H.; Hong, Z. Y.; Lin, J. D.; Hsiao, Y. C., Label-Free Multi-Microfluidic Immunoassays with Liquid Crystals on Polydimethylsiloxane Biosensing Chips. *Polymers (Basel)* **2020,** *12* (2).
27. Skaife, J. J.; Abbott, N. L., Influence of Molecular-Level Interactions on the Orientations of Liquid Crystals Supported on Nanostructured Surfaces Presenting Specifically Bound Proteins. *Langmuir* **2001,** *17* (18), 5595-5604.
28. Steel, A. B.; Levicky, R. L.; Herne, T. M.; Tarlov, M. J., Immobilization of Nucleic Acids at Solid Surfaces: Effect of Oligonucleotide Length on Layer Assembly. *Biophysical Journal* **2000,** *79* (2), 975-981.
29. Shen, J.; He, F.; Chen, L.; Ding, L.; Liu, H.; Wang, Y.; Xiong, X., Liquid crystal-based detection of DNA hybridization using surface immobilized single-stranded DNA. *Microchimica Acta* **2017,** *184* (9), 3137-3144.
30. Liao, S.; Qiao, Y.; Han, W.; Xie, Z.; Wu, Z.; Shen, G.; Yu, R., Acetylcholinesterase liquid

crystal biosensor based on modulated growth of gold nanoparticles for amplified detection of acetylcholine and inhibitor. *Anal Chem* **2012,** *84* (1), 45-9.

31. Humar, M.; Ravnik, M.; Pajk, S.; Muševič, I., Electrically tunable liquid crystal optical microresonators. *Nature Photonics* **2009,** *3* (10), 595-600.

32. Wang, Y.; Li, H.; Zhao, L.; Liu, Y.; Liu, S.; Yang, J., Tapered optical fiber waveguide coupling to whispering gallery modes of liquid crystal microdroplet for thermal sensing application. *Opt Express* **2017,** *25* (2), 918-926.

33. Duan, R.; Li, Y.; Li, H.; Yang, J., Detection of heavy metal ions using whispering gallery mode lasing in functionalized liquid crystal microdroplets. *Biomed Opt Express* **2019,** *10* (12), 6073-6083.

34. Wang, Z.; Liu, Y.; Gong, C.; Yuan, Z.; Shen, L.; Chang, P.; Liu, K.; Xu, T.; Jiang, J.; Chen, Y.-C.; Liu, T., Liquid crystal-amplified optofluidic biosensor for ultra-highly sensitive and stable protein assay. *PhotoniX* **2021,** *2, 18.*

Figure 1

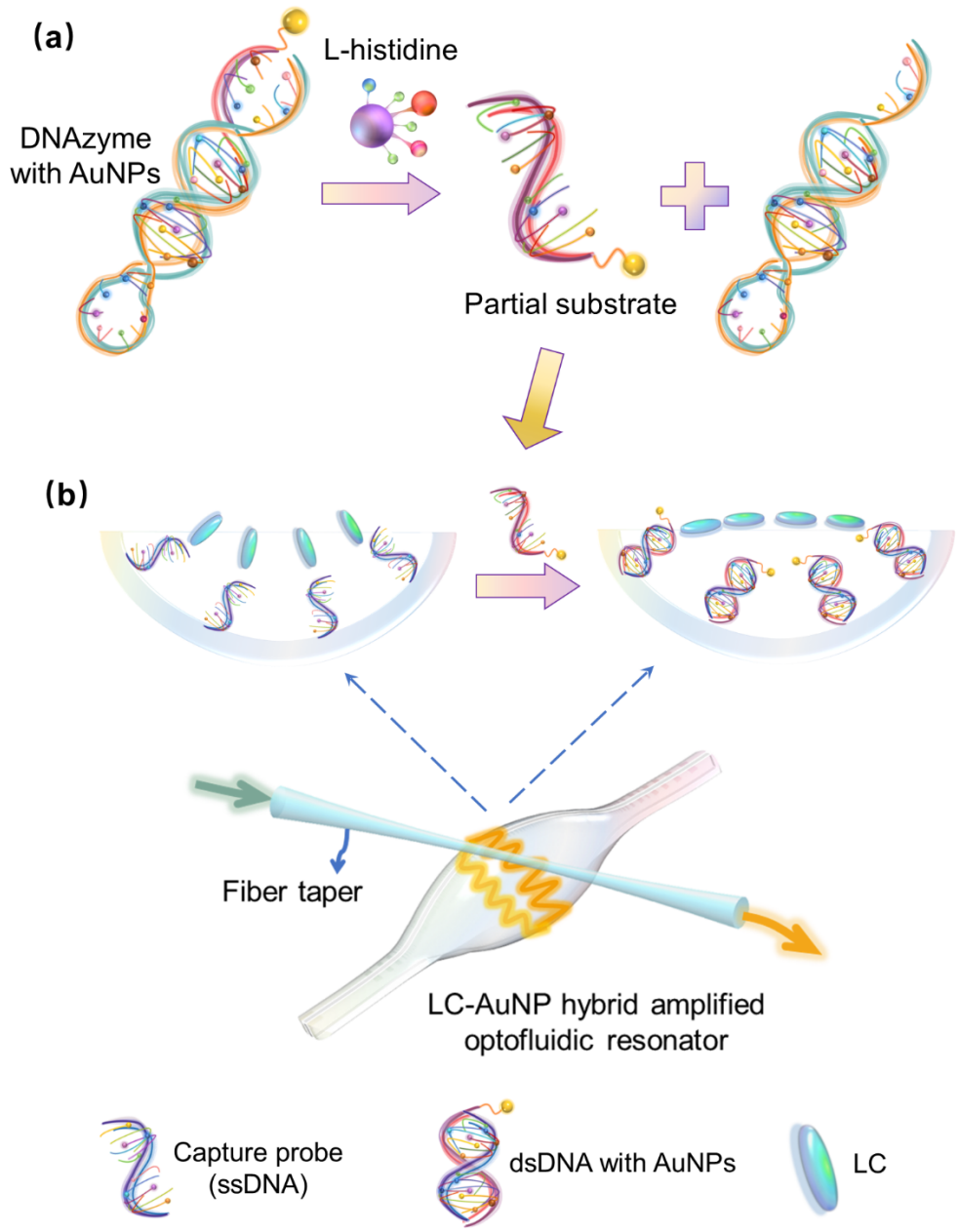

Figure 1 Schematic and principle of DNAzyme-based biosensor with LC-AuNP hybrid amplification for L-histidine detection. **(a)** DNAzyme can be specifically cleaved by L-histidine molecules and release the partial substrate (linked with the AuNP), which can hybridize with the capture probe (the complementary strand) to form dsDNA. **(b)** (Top) The capture probe immobilized on the internal surface of the microcavity can promote the homeotropic orientation of LC molecules. With the addition of the partial substrate and the formation of dsDNA, the surface topology was changed, and this led to the orientation transition of LC molecules from homeotropic to planar. (Bottom) Illustration of the transduction method of the DNAzyme-based biosensor by LC-AuNP hybrid-amplificated optofluidic resonator. The fiber taper was employed to produce WGMs.

Figure 2

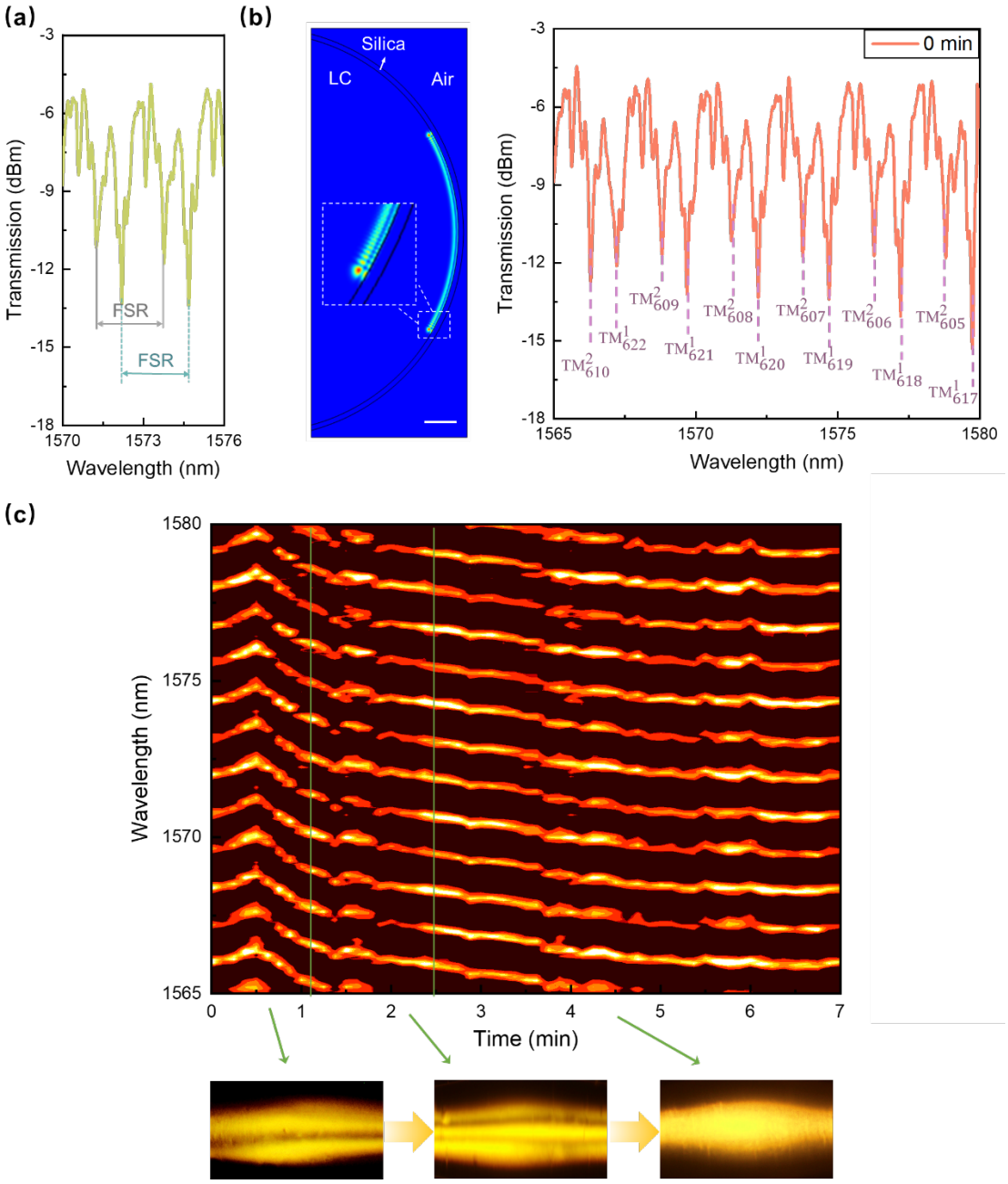

Figure 2 **(a)** WGM spectrum from LC-amplified optofluidic resonator, from which the FSR can be estimated to be 2.5 nm. **(b)** Electromagnetic profiles of WGMs supported by the DNAzyme-based optofluidic resonator with LC-AuNP hybrid amplification (left), and optical modes corresponding to the first-order TM polarization modes from 617 to 622 and the second-order TM polarization modes from 605 to 610 (right). Scale Bar: 15 μm. **(c)** WGM spectrum from LC-AuNPs hybrid amplified optofluidic resonator was continuously monitored for 7 mins at 5×10^{-7} M L-histidine. The wavelength exhibited red shift at first and then blue shift until stabilization. During this period, the polarized image of the microcavity also varied.

Figure 3

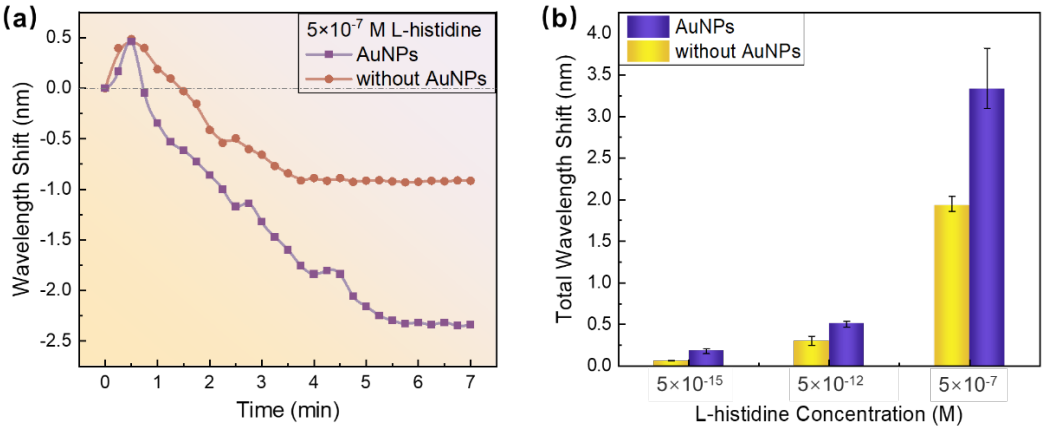

Figure 3 Effect of the AuNPs amplification technique on the DNAzyme-based LC biosensing platform. **(a)** Traces of WGM spectrum from the microcavity under 5×10^{-7} M L-histidine with/without AuNPs amplification. **(b)** Total wavelength shifts of WGM spectra from the sensing system under various concentrations of L-histidine (5×10^{-7} M, 5×10^{-12} M, 5×10^{-15} M) in the case of with/without AuNPs, respectively.

Figure 4

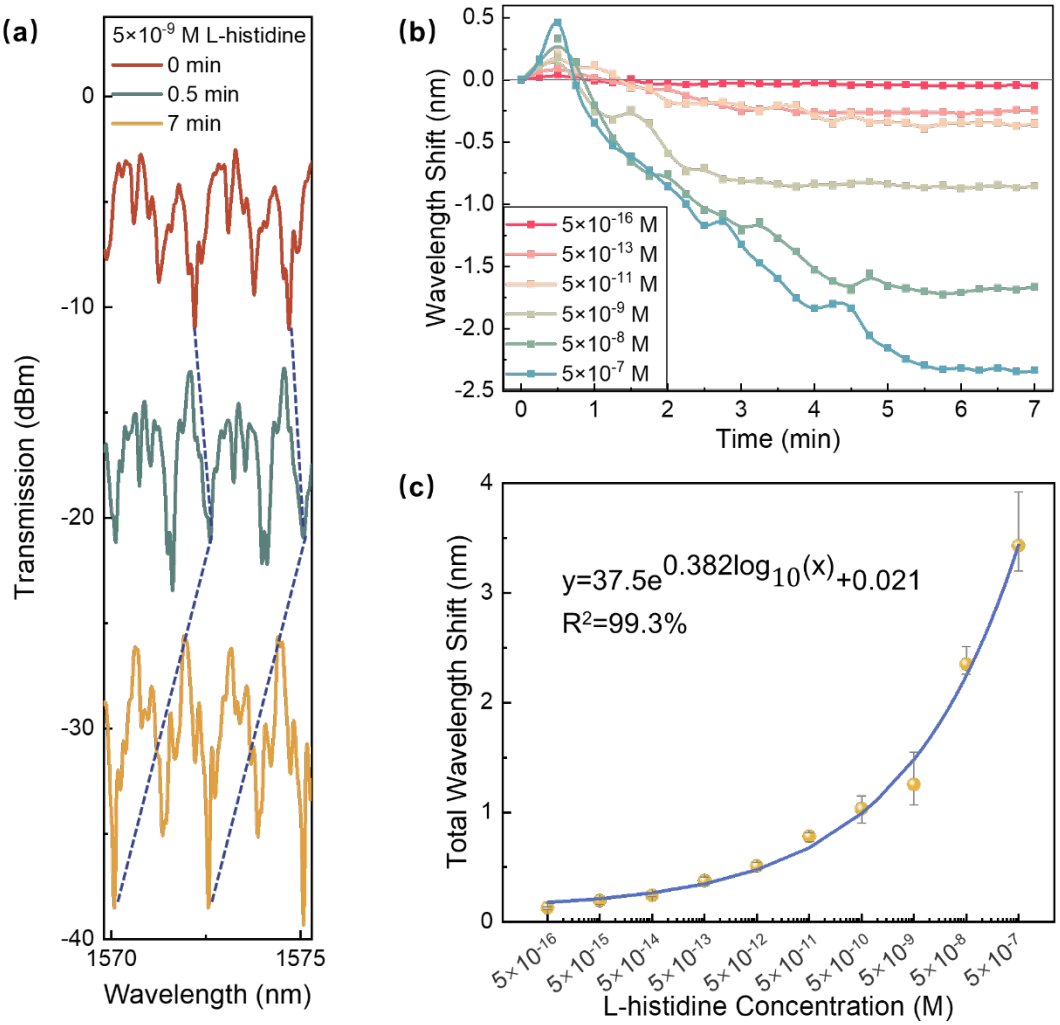

Figure 4 **(a)** WGM spectra of the LC-AuNP hybrid-amplified microfluidics after the addition of 5×10^{-9} M L-histidine at 0 min, 0.5 min, and 7 min, which triggered a red shift tendency at first and then a blue shift tendency until stabilized. **(b)** Real-time monitoring of the WGM spectral shift of the biosensor at various L-histidine concentrations over 7 mins. **(c)** Total wavelength shift as a function of L-histidine concentration from 5×10^{-16} M to 5×10^{-7} M in the semi-logarithmic plot (i.e., X-axis employed the logarithmic scale, Y-axis used the linear scale). The blue curve exhibited the calibration curve: $y=37.5e^{0.382\log_{10}(x)}+0.021$, $R^2=99.3\%$, where y represented the total wavelength shift, x represented the L-histidine concentration.

Figure 5

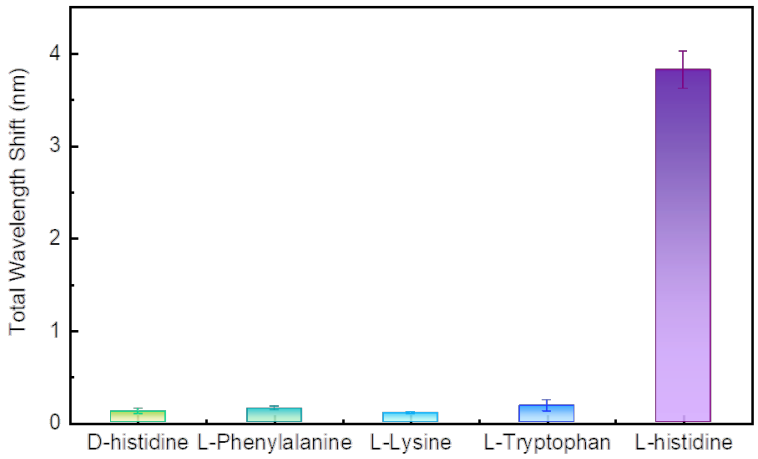

Figure 5 Relative spectral response of the DNAzyme-based, LC-AuNP hybrid-amplified optofluidic biosensor against different amino. (All other compounds have a concentration of 5×10^{-7} M).

Table 1 Recovery experiments of determination of L-histidine in urine samples. (n = 3).

Spiked (nM)	Found (nM)	Recovery (%)
0	6.72	-
1	7.62	98.7
5	12.09	103.2
50	59.16	104.3

Support Information

Capture Probe	NH_2-$(CH_2)_6$-TTTTTTCCGTCACATGATCTATGT
DNAzyme	SH-$(CH_2)_6$-AGATCATGTGACGGACATrAGGAAGAGATGTTTTTTTTTTCATCTCTTAACGGGGCTGTGCGGCTAGGAAGTAATGTCCTCC

Table S1 The synthesized oligonucleotides (5′-3′).

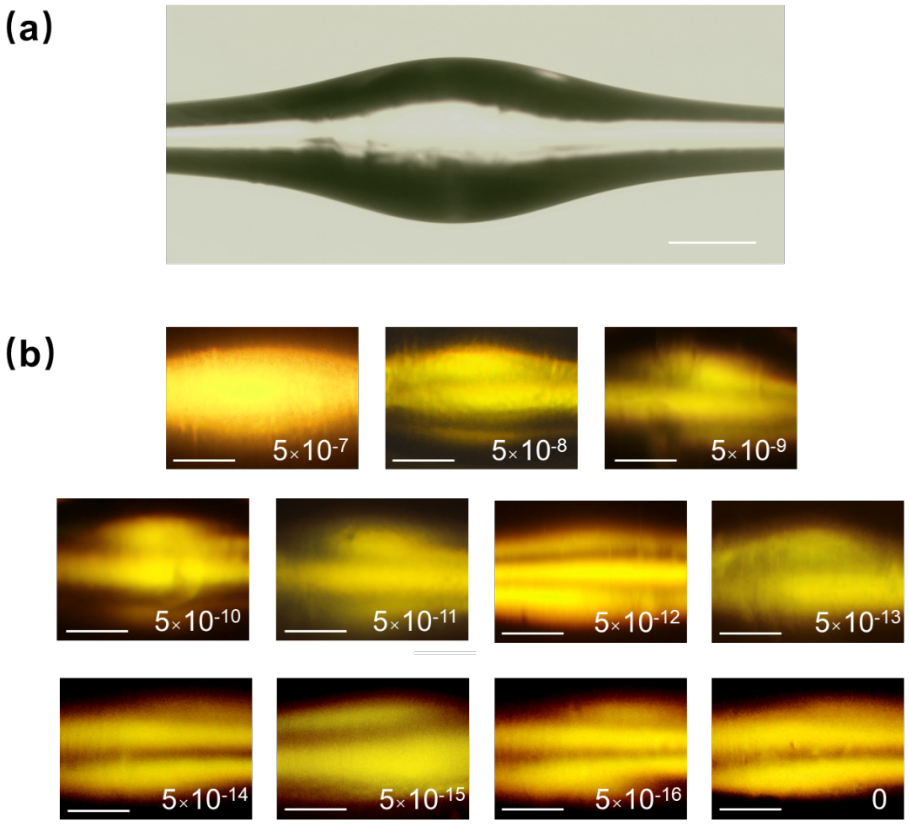

Figure S1 (a) Bright-field of LC-filled microcavity with a shape of microbubble. (b) Polarized images of DNAzyme-based, LC-AuNP hybrid-amplified microcavity under various L-histidine concentrations (from 5×10^{-16} M to 5×10^{-7} M, and 0 M as a control group). Scale bar: 100 μm.

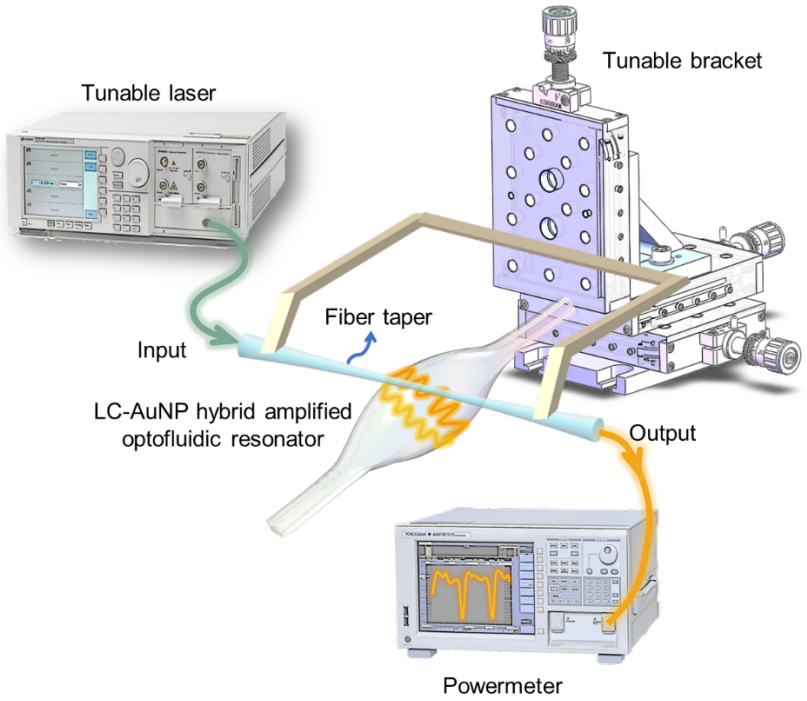

Figure S2 Illustration of the transduction method of DNAzyme-based biosensor by LC-AuNP hybrid-amplificated optofluidic resonator. To realize the phase matching and the efficient coupling, the tunable bracket was employed to adjust the gap between the micro-resonator and the fiber taper (as an evanescent-wave coupler). A tunable laser was guided to the resonator via the fiber taper to produce WGMs. Corresponding WGM spectral signals were recorded by the power meter.

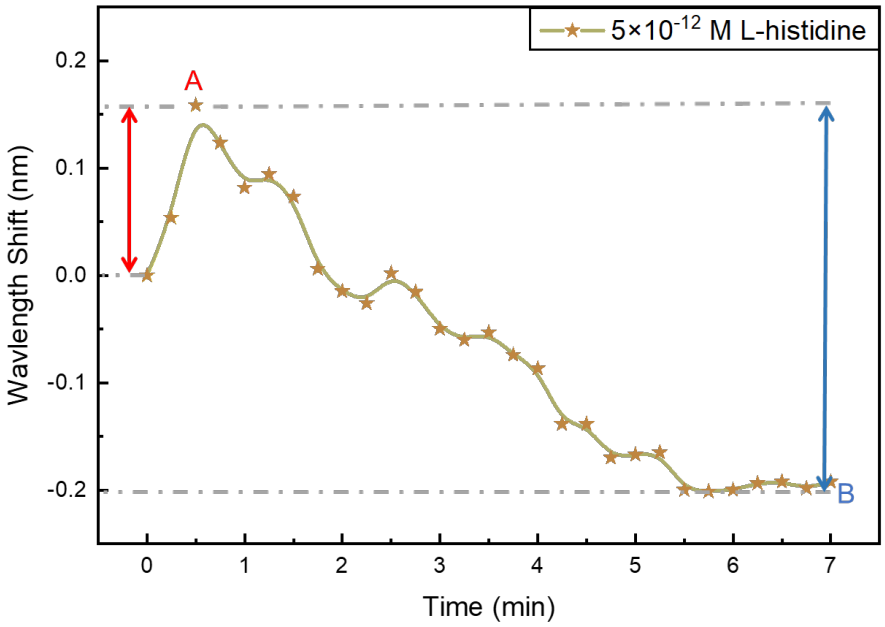

Figure S3 The definition of the total wavelength shift. The total wavelength shift can be calculated by the sum of the absolute value of the red-shift and the absolute value of the blue-shift. The red-shift equals the Y-axis coordinate of point A (i.e, the distance of the red line); The blue-shift equals the Y-axis coordinate of point A minus the Y-axis coordinate of point B (i.e, the distance of the blue line).

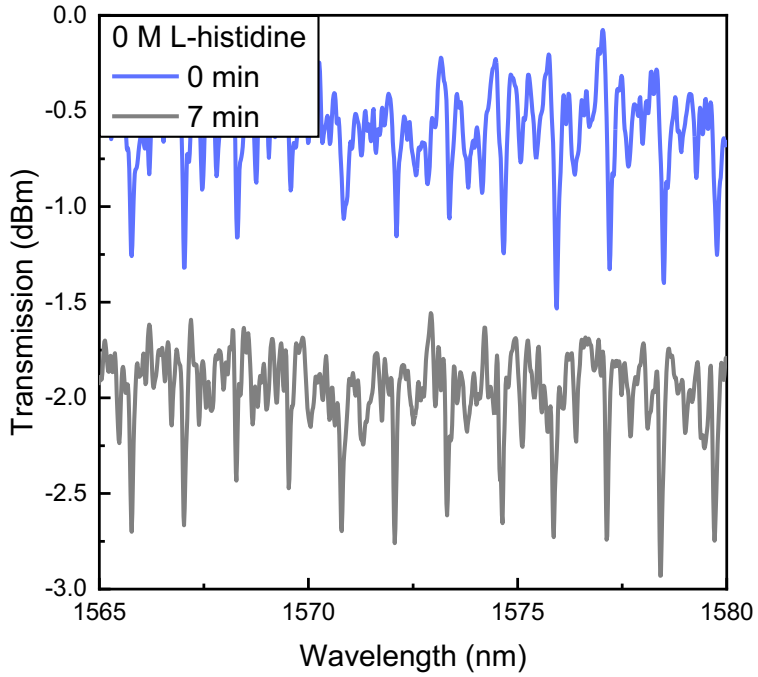

Figure S4 WGM spectral signal of LC-AuNP hybrid-amplified optofluidic biosensor under a control experiment (0 M L-histidine) at 0 min and 7 mins.

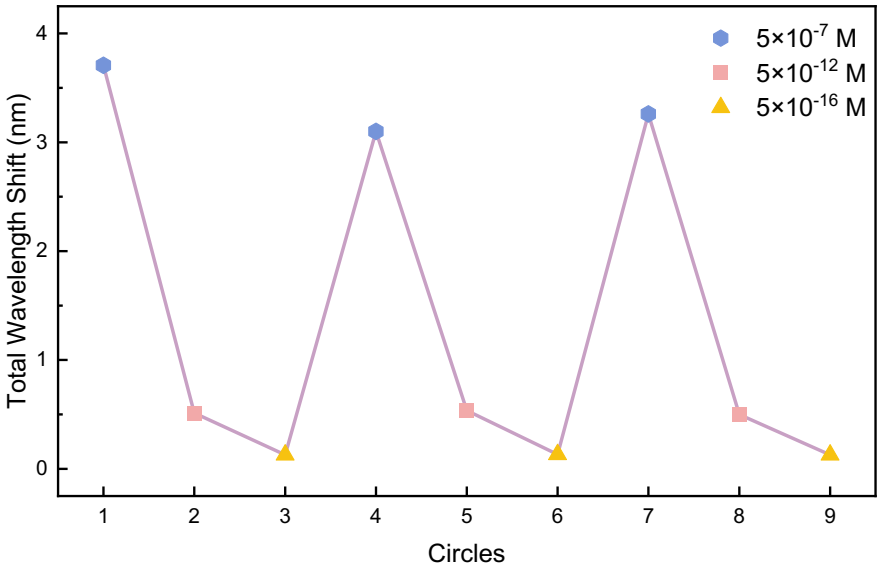

Figure S5 The spectral responses from the micro-resonator when it was continuously and cyclically exposed to different concentrations of L-histidine (5×10^{-7}, 5×10^{-12} and 5×10^{-16} M).